Supplement of The Cryosphere, 19, 975–995, 2025
https://doi.org/10.5194/tc-19-975-2025-supplement

The Cryosphere Open Access EGU

Supplement of

Understanding biases in ICESat-2 data due to subsurface scattering using Airborne Topographic Mapper waveform data

Benjamin E. Smith et al.

Correspondence to: Benjamin E. Smith (besmith@uw.edu)

S1. Impulse-response estimates from ground tests compared to in-flight transmit-pulse estimates from delay-fiber measurements

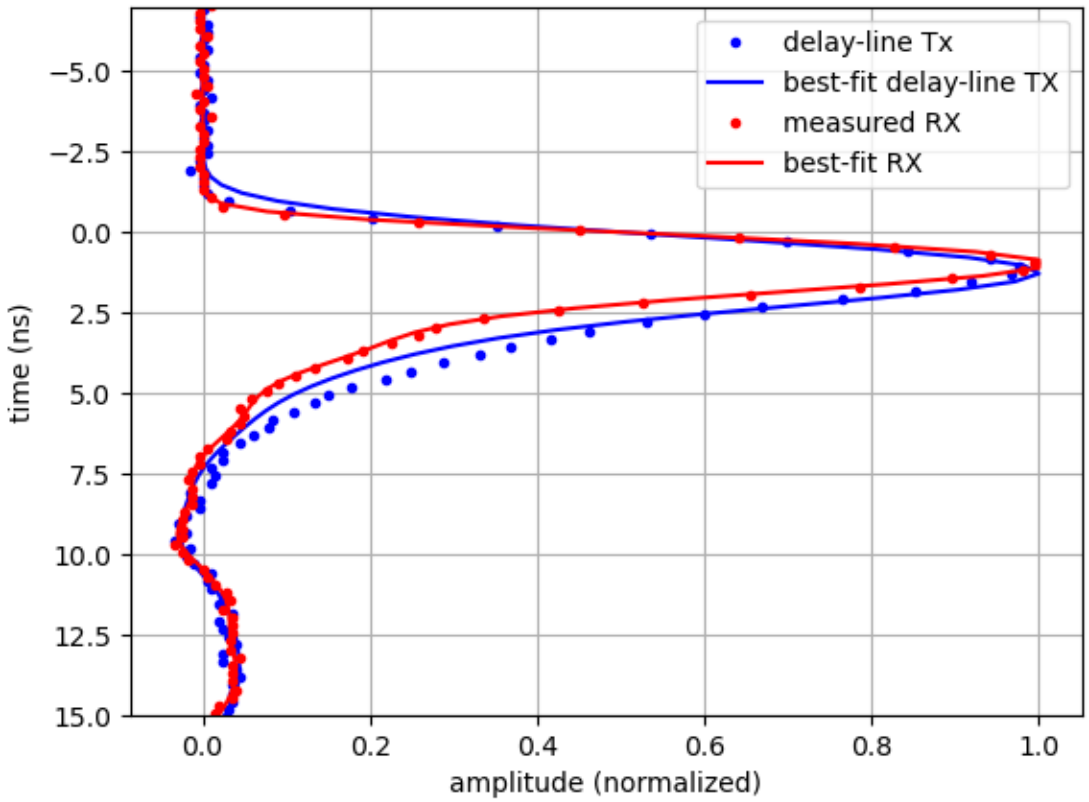

Figure S1. Comparison between sources of ATM impulse-response shape information. Plots show a return measured from a flight over the Kangerlugssuaq runway (measured RX), the waveform best fitting the Kangerlugssuaq return based on an impulse-response estimate from ground-test measurements (best-fit RX), the delay-fiber waveform for the same shot (delay-line TX) and the waveform best fitting the delay-line waveform based on the ground-test impulse response (best-fit delay-line TX). Each waveform is normalized to unit amplitude and is aligned on its first 50% threshold crossing.

We have three potential sources for information about the shape of the ATM transmitted pulse, each of which is summarized below.

1. Calibration measurements. Range calibrations for each ATM instrument and each campaign were established by recording waveforms with the laser pointed at a highly reflective calibration target (a Spectralon® panel). These waveforms give a record of the impulse response for a target that has minimal subsurface penetration. We calculated reference waveforms for each campaign by aligning several thousand pulses from each calibration file on their leading edges, normalizing them to unit amplitude, and averaging them.

2. Delay-fiber pulses. The ATM instrument diverts a small amount of laser energy from the transmitted pulse into an optical fiber, and then back to the detectors. This system records the shape of each transmitted pulse, but because the fiber allows multi-moded transmission, the measured pulses are blurred in time relative to the transmitted pulse. We have extracted
3. Surface-Return pulses. Over non-scattering surfaces, the returned pulses should be very similar in shape to the transmitted pulses. ATM often overflew the runway one or more time before landing, and the recorded pulse shapes give an estimate of pulse shapes that can be compared directly with the recorded transmitted pulses and the calibration measurements. However, because the laser beam was in general not perpendicular to the runway surface, we expect to see some pulse broadening due to the off-nadir angle of the beam.

Figure S1 shows a calibration waveform measured 27 March 2018, a surface-return waveform collected by the narrow-swath instrument over the Kangerlussuaq runway on 5 May 2018, and the delay-fiber waveform for the same shot. Each waveform is normalized to unit amplitude and aligned on its first 50% threshold crossing. The calibration waveform and the runway waveform are very similar, while the delay-fiber waveform is broader than either, with a full width at half maximum approximately 0.5 ns wider. We applied the fitting procedure to match the runway and delay-fiber waveforms with the calibration waveform, which reveals that the runway reflection matches the calibration waveform with no broadening or subsurface scattering needed, while the delay-fiber waveform requires broadening with a σ parameter of 0.76 ns to match the calibration waveform. The RMS misfit between the runway waveform and the calibration waveform is 1.1 digitizer counts, numerically equal to the RMS noise before the start of the pulse, implying that the runway waveform and the calibration waveform are, to within the precision of the ATM electronics, identical; by contrast, the delay-fiber return has an RMS misfit of 3.8 digitizer counts, likely reflecting the difference in skew between the two on the late-time side of the return.

The close match between the runway and calibration waveforms pulse suggests that the instrument impulse response is stable over at least monthly periods, and that it should be safe to assume that the transmitted pulse for each return is well represented by the calibration pulses. The broadening required to achieve a close match between the delay-fiber waveform and the calibration pulse is not inconsistent with the pulse being blurred in time by the multi-mode delay fiber, which would have allowed light propagating through the fiber to follow a variety of optical paths, leading to temporal broadening of the return. The converse hypothesis, that the delay-fiber measurement was an accurate representation of the transmitted pulse, would imply that the transmitted pulse was somehow narrowed in time during its interactions with the runway, and that this narrowing produced a waveform that matched the calibration waveform.

S2. Figure coordinates.

This paper contains three maps. The coordinates for the bounding box of each are presented in table S1, in the commonly used sea-ice polar-stereographic projection.

Table S1: *Corner coordinates for maps. This table gives corner coordinates for each map in the paper. Coordinates are in meters the NSIDC Sea-Ice polar stereographic projection (EPSG:3413).*

Figure	xmin	xmax	ymin	ymax
5	-701875	901625	-3401625	-598125
6A	-490992	-461013	-1304212	-1282714
8	-327563	-314763	-1570205	-1554459